



Photogrammetric 3D modelling and mechanical analysis of masonry arches: An approach based on a discontinuous model of voussoirs

B. Riveiro ^{a,*}, J.C. Caamaño ^b, P. Arias ^a, E. Sanz ^c

^a Department of Natural Resources and Environmental Engineering, School of Mining Engineering, University of Vigo, C.P. 36310, Vigo, Spain

^b Department of Materials Engineering, Applied Mechanics and Construction, School of Industrial Engineering, University of Vigo, C.P. 36208, Vigo, Spain

^c Geomatics Engineering Research Group, University of Leon, Spain

ARTICLE INFO

Article history:

Accepted 4 November 2010

Available online 3 December 2010

Keywords:

Close range photogrammetry

FEM

Masonry arches

Voussoirs model

ABSTRACT

This article shows the application of close range photogrammetry to the generation of accurate 3D geometric models for the subsequent evaluation of the condition state of historical masonry bridge arches by means of numerical analysis. The arch geometry in the model was obtained from each individual voussoir or ashlar with its own contour geometry, which was obtained by close range photogrammetry. From this precise geometrical model, mechanical modelling tools and finite elements analysis were applied to accomplish two main goals: to estimate the failure load considering the arch stability using a discontinuous model of voussoirs assembled without tension at the interfaces, and to obtain the distribution of stresses into each voussoir. The obtained results by means of this procedure are compared with those obtained by rigid blocks limit analysis with regular geometry.

© 2010 Elsevier B.V. All rights reserved.

1. Introduction

Masonry arches are one of the most common and extended structural shapes in the worldwide architectural heritage, given that they are present in domed buildings, vaulted tunnels, or historic bridges. Arch bridges are the greatest examples of the use of masonry arches. They are especially abundant in the Northwest of Spain because the irregular landscape topography and dispersion of settlements pushed the construction of infrastructures that allowed passing and communication. Hundreds of bridges dating from the Roman and Medieval periods are still in service and constitute a meaningful part of the road network as well as an important part of the heritage of engineering works, so they ought to be preserved and assessed.

Either because of their heritage value or their structural function in built up structures, the analysis of masonry arches is still the subject of numerous investigations [1–3]. However, their analysis is not a simple task. As pointed by Lourenço et al. [4], the geometric data are typically not available anymore; further, the workmanship and natural materials involve high variability of mechanical properties whose characterisation is usually difficult and expensive. Thus, there is no general analysis method for these structural elements. Two main approaches coexist: one focuses on structural behaviour analysis with finite element methods (FEM) [4]; the other is based on limit analysis theory or equilibrium analysis [5,6].

Masonry-bridge arches have two main characteristics that should be of interest to the scientific community. Firstly, their design has followed no standardised but empirical rules, and secondly, they have been subject to an increase in service loads through the years. In order to prevent the disappearance or degradation of these arches, the scientific community has to face, at least two questions: (i) development of reliable and affordable methods to document historical infrastructures, and (ii) improvement of the procedures of structural analysis and evaluation of the current structural condition of the bridges. The first question concerns the cultural value of each structure, and includes storing its metrical and graphical data. The second matter refers to the role the bridge plays on society, which makes the verification of its safety conditions a serious issue.

The bridge documentation and modelling can greatly benefit from high 3D digital imaging and processing techniques given the advances in surveying techniques, computer graphics hardware, three-dimensional modelling software tools, and 3D display capabilities. Virtual reconstruction of real world objects and scenes for further analysis is getting increasing interest in several fields as heritage [7], construction technology [8], medicine [9], and computer vision [10]. To obtain the geometry used for computations, photogrammetry and laser scanning techniques are of interest to several researchers in the fields of structure inspection and computation [11,12], especially photogrammetric techniques because they are more balanced in terms of cost and accuracy.

Structural computations might also incorporate geometric models obtained using digital modelling. While these models are derived from the external configuration of the structure (as ones obtained with traditional contact methods of measurement) with respect to

* Corresponding author. Tel.: +34 986 813 499; fax: +34 986 811 924.
E-mail address: belenriveiro@uvigo.es (B. Riveiro).

idealised regular geometric models, a higher degree of approximation to the actual geometry is reached, especially for irregular elements or highly variable geometry. Some recent research in this direction can be found in Macareno et al. where photogrammetry was used as a measuring tool in the analysis of the behaviour of a variable geometry structure [13]. Franke et al. demonstrated how photogrammetry shows a clear increase in the significance of strain distributions compared with conventional methods [14]. Arias et al. presented an approach to structural analysis based on photogrammetric models [15], and finally Schueremans and Van Genechten obtained the geometrical safety factor by limit analysis based on a terrestrial laser scanner (TLS) geometry survey of masonry vaults [16]. Some other interesting approaches for the use of photogrammetry in this field are described by Sonnenberg and Al-Mahaidi who used photogrammetry in lab tests to accurately measure the movement of concrete beams with shear reinforcement [17], by Mason who analysed the behaviour of structures with variable geometry [18], and by Jauregui et al. who used photogrammetry for bridge inspections [19].

This paper presents a methodology to obtain 3D models from digital close range photogrammetry to generate a precise geometric documentation of the structure under study for further structural computations based on the finite elements method using mechanical modelling tools. A method to determine the failure load of masonry arches using a discontinuous model (micro-model) is presented. The model of each voussoir is made from the precise geometry of its external faces obtained by photogrammetric measuring and surface processing tools. The methodology is applied to the Cernadela Bridge (Fig. 1). The structure is located in the municipality of Mondariz, in Northwest Spain. Dating from the 15th century, it is thought that the Cernadela Bridge in its present form was raised on the remains of a Roman bridge.

2. Theoretical grounds

2.1. The photogrammetric survey

Image-based measurement techniques play an important role in virtually all natural sciences and engineering disciplines since they can provide amount of qualitative and quantitative information and knowledge about observed objects in a global, non-contact way with high spatial resolution. But the application of this technology to bridges modelling and documentation has just recently started to be accomplished (see [19]) probably due to the structural complexity of this kind of constructions. This specific application requires a particular methodology in data collection and data processing. In this study, a digital monoscopic system has been employed because it might be still considered more feasible in heritage documentation applications in terms of cost-efficiency balance than stereoscopic photogrammetry, automated image matching procedures, or even laser scanning surveys. The existence of low cost photogrammetric platforms like Photomodeler Pro® makes it easier for photogrammetry to be developed by non experts in geomatics. Photomodeler Pro® works on the basis of convergent monoscopic photogrammetry. This way with only 3 images of one object its geometry can be modelled. Stereoscopic systems are usually more expensive and require of more advanced knowledge about the technique.

The principles of close range photogrammetry have been frequently reported. A brief overview is given here for a better following of the proposed methodology. The final goal of a photogrammetric process is to obtain a set of 3D coordinates of points on the surface of the object in order to build 3D digital models of the object that represent its geometry. Images are obtained from camera positions all around the object [20]. Camera axes are usually highly convergent [11]. The position of a point in space is commonly defined by a three-dimensional Cartesian coordinate system. The origin, scale and orientation can be

arbitrarily defined. It is often necessary to convert between coordinates in systems having different origins, orientations and possibly scales.

Coordinate transformations may be divided into three steps: translation, rotation and scale change. The origin of the primary x', y', z' axes is translated by $T (T_x, T_y, T_z)$, the scale along each axis is multiplied by K and the axes are given sequential rotations ω, φ, κ . After these three steps the original $x', y',$ and z' axes are transformed into secondary $x, y,$ and z axes. In summary, seven parameters define the transformation: $T_x, T_y, T_z, \omega, \varphi, \kappa,$ and K (see Ref. [21] for further information).

The starting point for building a functional model for close range photogrammetry is the central perspective projection, which uses the collinearity equations to estimate the object coordinates (on the object surfaces) from the known image coordinates (in the pictures); [22] provide more information.

A multi-station convergent bundle adjustment gives higher quality results when the pictures of different or the same cameras are used. In a bundle adjustment, all measured photo-coordinates are processed simultaneously using iterative linearised least quadratics methods to evaluate the exterior and interior orientation elements, camera calibration data and object space coordinates [23]. In Arias et al. [24] a functional model of the photogrammetry based on collinearity equations was shown. In this model the parameters to be estimated, the measured points and the elements whose values are known constants are incorporated. If no prior calibration values of cameras have been obtained, it is possible to include calibration elements in the unknown parameters only. This procedure is referred to as self-calibration [25].

One of the advantages of current digital photogrammetric work stations is that they introduce automatic estimations of the adjustment quality. Thus, the precision of the virtual 3D model can be reported as the standard deviation of the estimated coordinates for each point that defines the boundaries of the object. The resulting values depend on many factors, especially the geometry of the individual shots and the redundancy level of the measurements.

Finally, it might be highlighted that the 3D models (point clouds and line models) obtained from photogrammetry reproducing the actual geometry of individual elements and sets of complex geometries can be exported into computer aided design, manufacturing and engineering software (CAD-CAM-CAE). This kind of software include highly specialised surface processing tools along with mechanical analysis (with kinematic relationships between solids and finite element analysis) that allow the processing of complex surfaces and solids and the creation of sets of parts that can be processed for analysis using finite element software package. Furthermore, they include the possibility of exporting the generated model to a more specialised structural analysis program.

2.2. Structural modelling and analysis

The basis for the formulation of plastic analysis (or mechanism methods) applied to masonry arch structures was established by [26] and [5,6]. This formulation can be posed in terms of the thrust line, whereby the failure of the structure occurs when the thrust line touches the boundary of an arch geometry, which forms joints in a sufficient number of points to convert the element into a mechanism. More recently in [27,28] computer-discrete formulations have been used: the model consists on a series of rigid blocks to idealise the behaviour of the voussoirs of the arch. The problem can be raised in terms of equilibrium or kinematic, in which case it can be resolved by linear programming in many cases.

Furthermore, other approaches may be used based on finite elements, discrete elements or hybrid (combined) methods of finite and discrete elements [29]. To determine the load capacity of masonry arches, such methods generally require iterative processes. Information about numerical modelling methods for masonry structures can be



Fig. 1. Upstream view of the Cernadela Bridge, in Mondariz Council, Spain. Arches are numbered from left to right.

found in [4]. In summary, two types of models can be identified: discontinuum models (also called micro-models), in which units and interfaces (and mortar if it exists) are represented individually, and continuum models (or macro-models), in which masonry is represented by a homogeneous continuum that includes units, mortar and interfaces.

In this case, a discontinuous model (micro-model) is used to determine the failure load in existing masonry arches. This model is made from the precise external geometry of each voussoir obtained by photogrammetry. The interfaces are in direct contact between the units of stone with no mortar in the joints, and they do not transmit tension. The failure load can be estimated [4] from the load–displacement diagram (or separation between voussoirs), which can be obtained by varying the loads in an iterative process by determining the peak load. In each voussoir and for each load level analysed, a finite element discretisation is performed, and the stress distribution inside and at the interfaces is obtained.

3. Photogrammetric 3D modelling of a bridge arch

3.1. Instrumentation

The described methodology has been applied to the case of the medieval bridge of Cernadela, which is located in the council of Mondariz in the region of Galicia, Spain (Fig. 1). The photogrammetric survey of the Cernadela Bridge was executed with a digital camera (Canon EOS 10D). The camera is the most important element in a photogrammetric measurement system. Traditionally, customised metric cameras manufactured especially for photogrammetric measurements are used. Unfortunately, the high cost of metric cameras restricts the wide application of close range photogrammetry. The use of high-end, commercial off-the-shelf digital cameras allowed for high accuracy measurement.

This camera model has an RGB CMOS (complementary metal oxide semiconductor) sensor with a resolution of 6.3 megapixels (3072×2048 pixels). CMOS sensors were previously used only for low level digital cameras [30]. With the improvement of its properties, the CMOS sensor is now employed in high-end cameras at a much lower price than those with CCD sensors. The main difference between a CCD and a CMOS

sensor is that the former processes image pixels in sequence (pixel by pixel), while the latter processes pixels simultaneously. As a result, CMOS sensors provide higher speed at a lower price and use much less space and energy.

This camera was equipped with a Canon EF 20 mm wide-angle lens. Wide-angle lenses are those whose focal length is below 35 mm; they have a wider field of view that simplifies (minimises) data acquisition. The data acquisition was achieved using the manual focus set at the infinite position, ISO 100, and automatic exposure. A set of circular paper targets were used as orientation points, and the coordinates of their mid-cross-point were determined with a Leica X-Range 1102 laser total station. The Photomodeler 5.0 photogrammetric workstation was used.

To convert the Photomodeler files, CAD software was used. Then this model was converted into a 3D design with a normalised format. The mechanical modelling of the arch was executed in Catia V5. To compare the model results, LimitState Ring 2.0 [31] structural analysis software was used.

3.2. Sensor calibration

As previously explained, an important advantage of the bundle adjustment system is that it permits the evaluation of elements of camera calibration and interior orientation together with the exterior orientation parameters and the object space coordinates. Another option consists of performing a calibration procedure with photographs of a calibration field, where the coordinates of the points in the object space are measured with micron-order accuracy. As a result, the principal distance and the position of the principal point, as well as the constants that correspond to the radial symmetric distortion of the lens,

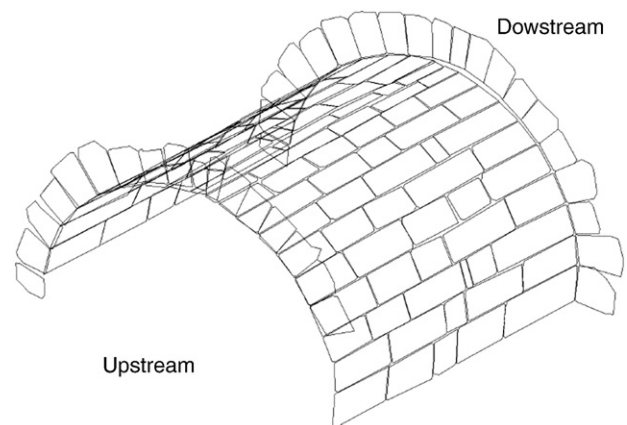


Fig. 2. Wireframe model of arch 2 obtained from photogrammetric process. It is viewed from upstream side.

Table 1
The 3D model accuracy with 95% confidence levels.

Object accuracy	
X (m)	0.0696
Y (m)	0.00849
Z (m)	0.00472
RMS (m)	0.01195
RMS (pixel)	1.22

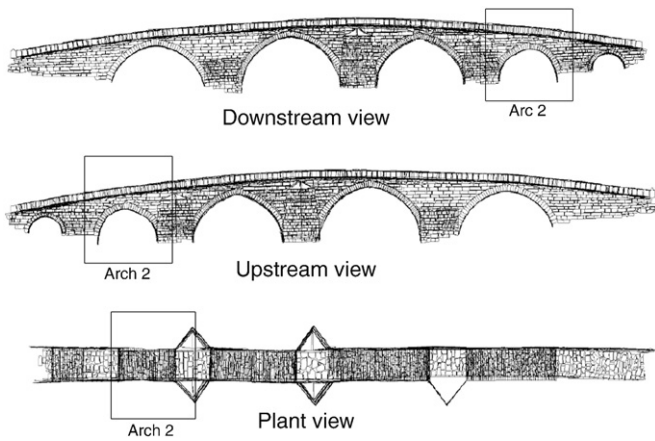


Fig. 3. Wire frame model: scaled plan views of the Cernadela Bridge (upstream front view, downstream front view, top view).

are estimated. The calibration of the camera used in this survey was performed with the calibration module of Photomodeler Pro. This procedure consists of making between 8 and 12 photographs of a calibration pattern. Then by means of the bundle adjustment of the rays of the points printed in the pattern, it is possible obtain the internal orientation parameters of the camera. The values obtained for the Canon EOS 10D calibration are described in Ref. [24].

3.3. Data acquisition

This step was performed following the principles of convergent multi-station systems:

- Multi-station network design. The placement of camera stations must avoid obstructions in the bridge walls, and ensure optimum visibility of the ashlars. The maximum distance from the camera to the wall is estimated as a function of the expected average precision of the feature measurements, the expected image measurement coordinate precision, the number of photographs at each station and the principal distance of the camera; Ref. [18] provides more details. The second parameter to take into account is that the points that are defined in the object space, which are used to perform the restitution of points over the stone surface, are rock features (mainly crystals); these are not punctual elements, so low precision in the image coordinate measurement might be expected.
- Topographic support: control point measurement. Reference targets might be used to accurately measure the coordinates in a global coordinate system to scale and level the resulting model.
- Image acquisition. Parameters to be considered according to Ref. [24]: adequate lighting of the photographed object; given the size of the object, the image may be gathered as overlapped models (portions of the bridge); there must be at least 50% overlap between photographs.

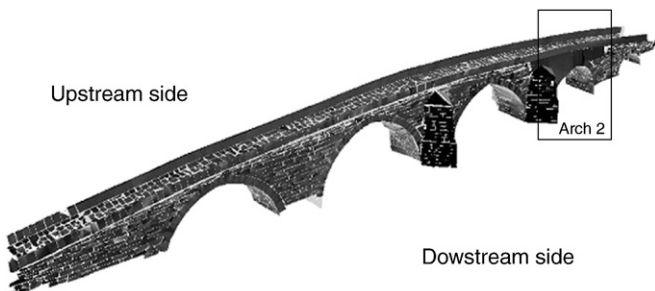


Fig. 4. Surface 3D model of the Cernadela Bridge (perspective view from downstream). In the right of the picture is the second arch where mechanical analysis was performed.

Table 2
Mechanical properties for materials.

Young's modulus	E [N/mm ²]	23 · 10 ³
Poisson ratio	ν	0.2
Masonry unit weight	γ [kN/m ³]	20
Backfill unit weight	γ [kN/m ³]	15
Tensile resistance for masonry	σ [N/mm ²]	0

The camera–object distance ranged between 5 and 12 m in the Cernadela Bridge survey. Reference targets with a 10 cm diameter were used to accurately measure the coordinates in a global coordinate system to scale and level the resulting model.

3.4. 3D modelling

This process was performed according to the following steps [23]:

- Relative orientation of the photographs. Position and orientation of the camera poses in the object space are estimated thorough the image coordinates of control points in convergent images on the base of the collinearity equations.
- Absolute orientation of the model. The whole model is levelled and scaled through the control points whose coordinates were measured by total station.
- 3D modelling. The reliability of the final 3D model lies in this step. Given the complexity of the task, the definition of the 3D model as a cloud of restituted points is considered the most reliable method. The image coordinates in convergent shots are obtained for points on the boundary and walls of the bridge for subsequent computation of the corresponding coordinates in the object space on the basis of the collinearity condition and a least squares adjustment.

The 3D model of the Cernadela Bridge contains 25,058 points; 160 photographs and 100 control points were used for the modelling process. The final average accuracy of the coordinate estimation in the object space is shown in Table 1.

The influence of redundancy in the RMS is well documented. For this work, the image coordinates of each point in three or four photographs were used to estimate the corresponding coordinates of the points in the object space; they had errors between 9 and 12 mm.

Based on the cloud of restituted points, two other models were created in Photomodeler: a wire frame model and a surface model. The wire frame model of the whole bridge with corresponding plan and side views (Figs. 2 and 3) was used to generate solid models with the overall geometry of the bridge in CAD format, which require selecting a reduced number of points to define this geometry. The surface model was built using 4587 surfaces (Fig. 4), and this model was used to locate cracks and other structural defects of the Cernadela Bridge.

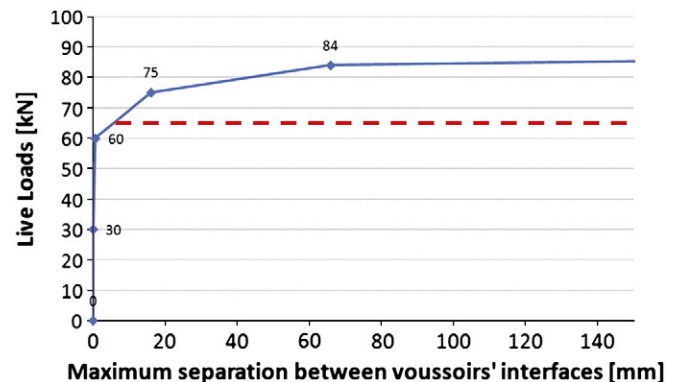


Fig. 5. Live load versus separation between voussoirs diagram. Cernadela Arch model with proposed method.

Table 3
Separation versus live load.

Load (kN)	Separation (mm)
Own weight (OW)	0.0012
OW + Backfill (B)	0.00344
OW + B + 30 kN	0.061
OW + B + 60 kN	0.66
OW + B + 75 kN	16.1
OW + B + 84 kN	65.9
OW + B + 90 kN	481
OW + B + 300 kN	$5.13 \cdot 10^5$

The main dimensions of the bridge are:

- Length of spans (left to right, front view): 3.58 m; 6.56 m; 10.01 m; 11.14 m; 10.30 m.
- Height of piers (left to right, front view): 3.95 m; 3.87 m; 4.19 m; 4.16 m.
- Rise of arches (left to right, front view): 1.79 m; 3.77 m; 5.22 m; 5.80 m; 4.75 m.
- Width (max) of piers (left to right, top view): 3.89 m; 3.82 m; 3.92 m; 3.90 m.

4. Mechanical modelling of an arch ring

The CAD wireframe model obtained as a result of the photogrammetric process was used to separate each voussoir into individual units by identifying the edges of their visible faces. Each voussoir was then converted to a design standard format (STEP format) to be imported from mechanical design software (Catia V5), where the external surface of each voussoir was created using the identified faces. Each voussoir was generated from the visible edges of the external arch ring. The rear face of the voussoirs was defined by the projection of the front face's lateral edges on a perpendicular plane to the lower face. The rest of the faces were completed from the available edges.

No test has been available for the non-visible internal areas of the bridge for this work. In recent years some advances have been reported in non-destructive techniques for obtaining non-visible geometric data. In this field, the work of Fernandes [32] on ground penetrating radar, Solla et al. on GPR simulation techniques [33], or Colla et al. 1997 [34] on sonic methods can be found. Orbán [35] sorts the following testing techniques according to their ability to provide reliable and quantitative geometric data (in decreasing order of reliability and quantification capacity): coring and analysis of cores and boroscopy, georadar and

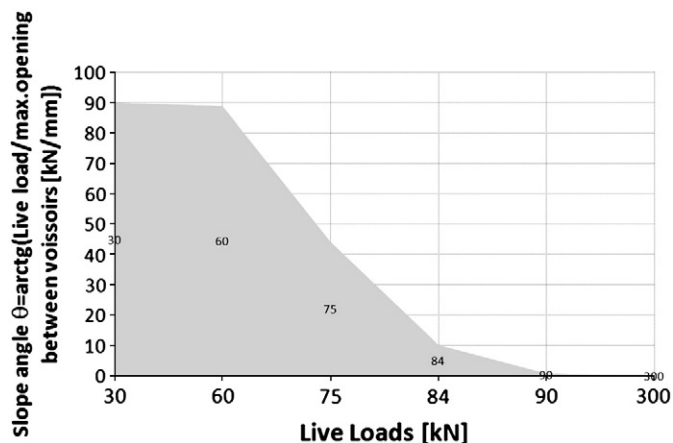


Fig. 6. Slope angle of live load versus maximum opening between voussoirs diagram.

sonic methods, conductivity measurement and infrared thermography (this last one only in some precise cases).

The solid model of each voussoir is generated independently while considering the width defined for the calculated arch ring. The complete model is formed by assembling all the individual voussoirs that form the arch and defining the material and contact interface properties.

The stress and strain analysis by finite elements has been carried out in the cases analysed in this work in module 'Generative Structural Analysis' of Catia V5. The contact between voussoirs was modelled with restrictions (constraints) that only allow the transmission of compressive stress. The following hypotheses have been considered. The first three are consistent with limit analysis typical hypotheses [6].

- The compressive strength in stone voussoirs is not limited a priori. Stress distribution generated by the failure load will be obtained by finite element analysis.
- No tensile strength is considered between the voussoir contact interfaces. Opening of joints between voussoirs without tension is allowed.
- Sliding between voussoirs is not allowed.
- The voussoirs may deform elastically. Not changes have been considered in the elastic parameters values during the load process.
- Direct contact occurs between the stone voussoirs without fill at the joints.
- Arch ductile behaviour is assumed. The effects of previous applications of loading are ignored. Loads and load increments are statically applied.

5. Finite elements modelling and failure analysis

5.1. Discontinuous model of voussoirs for analysis by finite elements

The model seeks to adjust the actual geometry of external voussoirs of the arch being analysed. The geometry corresponds to the actual shape of the bridge, with deformation measured in situ. The model obtained in the pre-process stage can be exported to various programs for the finite element processing stage.

Each individual model voussoir was discretised into finite elements. Ten-node parabolic solid tetrahedrons with 4 nodes at the vertexes and elastic behaviour were used. Three degrees of freedom (translation) per node were considered, which reduced the computing time at the expense of somewhat reducing the calculation accuracy (stresses and strains in the voussoirs). Contact defined between voussoirs allows connection of a finite element mesh node with the face of a contiguous element. The behaviour of the union is established from the projection of a node of the model (the slave node) onto the surface that is defined by a series of master nodes of its environment and the neighbouring voussoir. The separation between the slave node and the projected point is defined, which corresponds to the initial separation between voussoirs. As indicated above, in this case, direct contact is considered with zero initial separation without filling in the joints and, therefore, without tensile strength. Rotation is permitted between voussoirs, but not relative sliding.

The second arch of the Cernadela Bridge was selected as an example for this application. The complete arch model consists of a total of 30 assembled voussoirs. A total of 1994 elements and 3128 nodes were considered in the whole model. The nature of stone used in the bridge is granitic. This type of material is frequent in this region, according to its geological characteristics. However, the precise characterisation of the mechanical properties for the material is complex and usually requires testing. The values used are purely illustrative, in order to explain the methodology. The material characteristics considered are shown in Table 2.

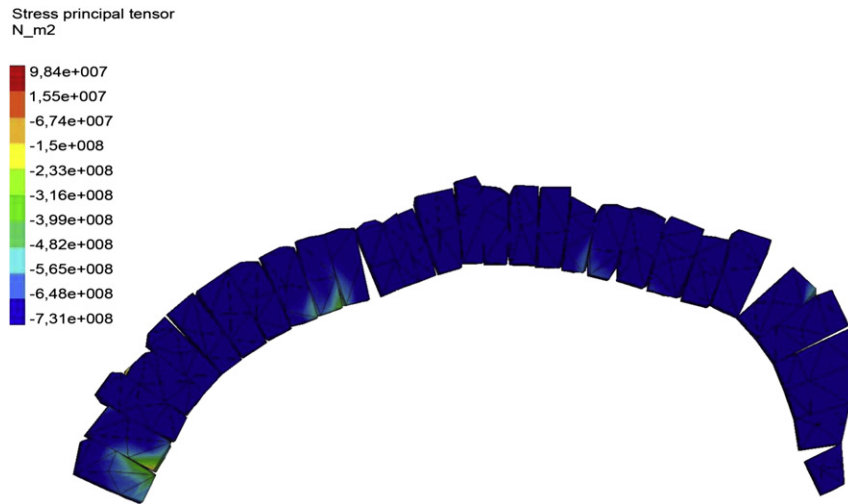


Fig. 7. Discontinuous model of voussoirs for failure load estimation of Arch 2 in the Cernadela Bridge.

5.2. Estimation of failure load

In methods of calculation based on the thrust line [6], failure is caused by the formation of a mechanism with a sufficient number of hinges. The hinges are located at points of contact between the thrust and physical edge line of the arch. In the numerical analysis performed in this work, self-weight and backfill loads were introduced in addition to a concentrated live load located at a distance of $\frac{1}{4}$ of the arch span away. The value of this live load was gradually and iteratively increased in successive calculations by tracking the evolution of maximum nodal displacement (and the maximum separation between voussoirs) versus live loads. During the iterative process of live load variation, the rotations were concentrated in a series of joints between voussoirs. Thus, the model shows a tendency to form hinges in a series of interfaces. The appearance of hinges in a sufficient number of points after a certain load value causes the arch to become an unstable mechanism. When the live load is close to failure, there is significant displacement variation and separation between voussoirs, which produces a quick change in the slope in the load–displacement graphic, and the deformations grow rapidly against the loads. The load related with this change of slope in the diagram can be considered to be a failure load estimation, which is obtained, in this case, with an accurate geometric photogrammetric model.

For the case study, an external single arch ring with a width of 500 mm was considered. Therefore, the failure load could be obtained by the unit of width for uniformly distributed loads across the barrel width. The live load was applied directly over the extrados side of the voussoir located at the quarter span. Dispersion through the fill was not taken into account for the load distribution over the arch ring. The arch–backfill interaction and the passive pressures were not considered in this model. Therefore, the expected results for the load factor are considered conservative in accordance with the hypothesis. A multi-span failure mechanism can also typically occur in multi-arch bridges, especially in segmental arch cases with slender piers. In Fig. 5, the load versus maximum separation between voussoirs can be seen according to the results shown in Table 3. In the figure, the change in the slope in the diagram (continuous line) can be seen. In this case, the change of slope can be considered significant for live loads exceeding values of about 75 kN, as can be seen in Fig. 6.

A simplified model with regular geometry of the second arch of the Cernadela Bridge was analysed with Ring 2.0 [31]. This software tool is designed specifically for the analysis of masonry bridge arches using the rigid blocks method. The backfill options were chosen in the

program to consider the same role over the load distribution and the passive pressures than in the previous model (no load dispersion and no passive pressure). The failure live load obtained in this way, in the same position, was 65.6 kN. This result is represented by discontinuous line in Fig. 5.

In Figs. 7 and 8, it is possible to appreciate the formation of hinges in similar positions in both cases: the arch with accurate geometry and the one with simplified regular geometry. Fig. 9 shows at its top the contact surfaces between voussoirs, for the arch area with maximum separation represented below. In the colour scale shown at right, openings obtained between the voussoirs are illustrated. The situation in the figure corresponds to the failure live load of 75 kN.

The load factor obtained by both methods differs by 12.5% in the case analysed. It is noted that both methods use different geometric models: closer to reality in the numerical method and a simplified ideal geometry in the second method. Furthermore, in the numerical method the loss of stability occurs in a gradual process around a short range of load values. It is also necessary to note that the accuracy in the numerical method depends on the number of iterations performed around the change of slope in the diagram.

5.3. Stress distribution inside the voussoirs

The stress distribution within each voussoir is obtained for the failure load. The use of elastic finite elements to represent material behaviour inside voussoirs was considered to be acceptable, taking into account that stress levels for instability load failure are often relatively low for stone arches and the contact interfaces between voussoirs allow opening without tension. Checking the material crushing condition

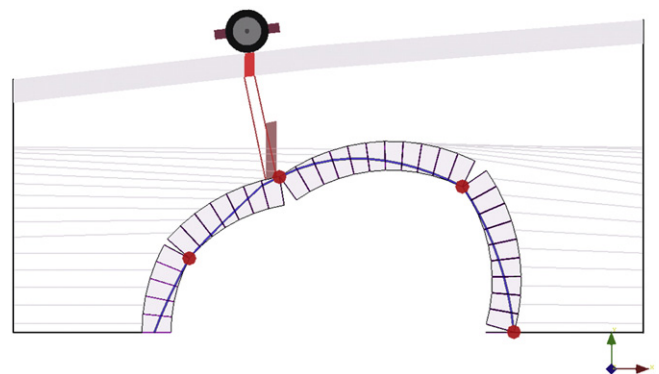


Fig. 8. Analysis model of Arch 2 in the Cernadela Bridge with Ring 2.0 software.

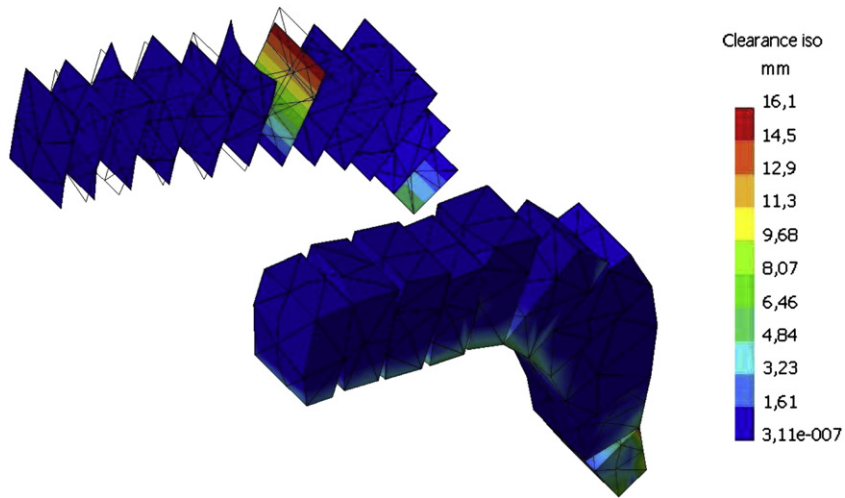


Fig. 9. Separation at interfaces between voussoirs.

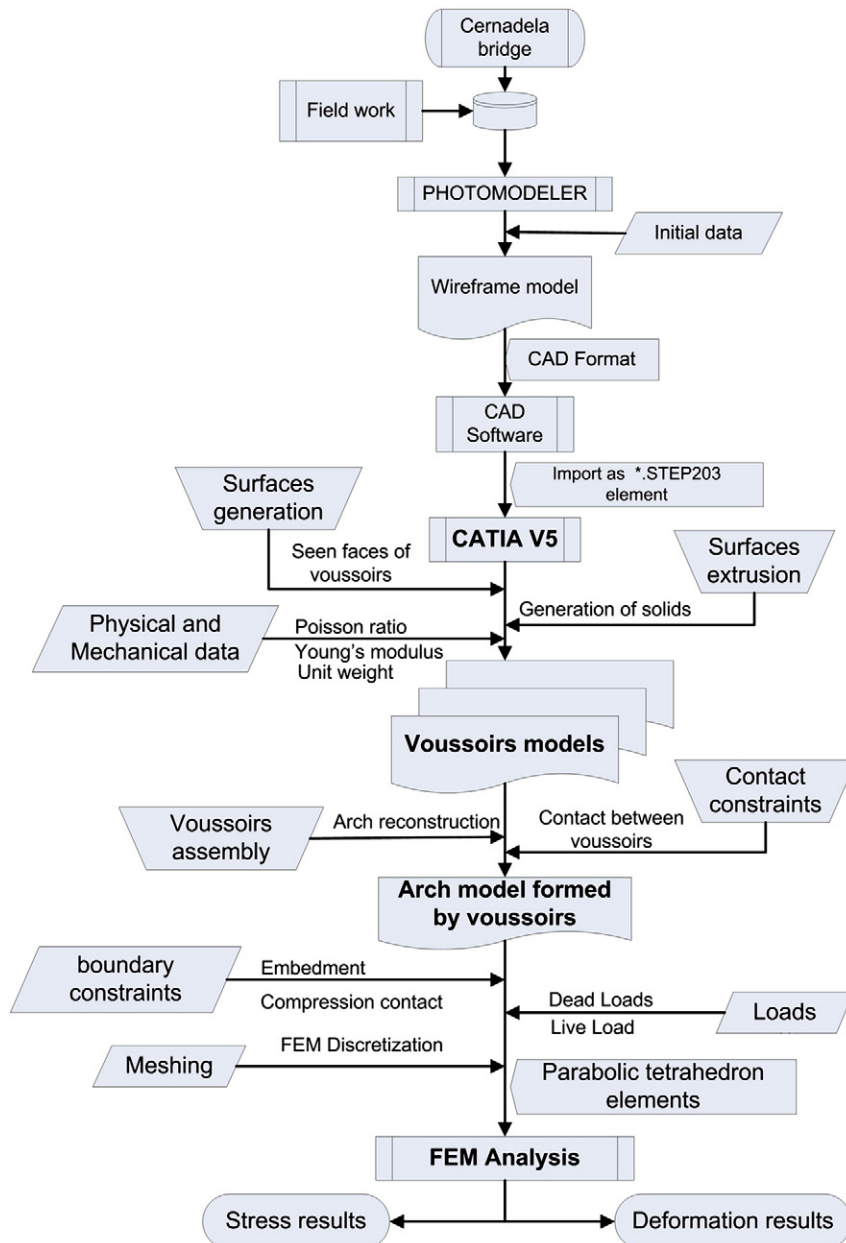


Fig. 10. Process flowchart.

would be possible in the case where results from tests were available. The Mohr–Coulomb failure criterion is recommended for the case of brittle materials such as stone, as in this case. The whole flowchart for the complete process is presented in Fig. 10.

6. Comparison of results with rigid blocks analysis and ideal regular geometry

Results of comparative studies carried out between the method used in this paper and other analytical methods for failure load obtaining in masonry arches are presented below. The geometrically regular arch studied by Loureço in Ref. [4] was taken as reference. This author makes a comparative analysis of the results of the same semicircular arch with several different methods, including linear elastic finite element analysis (eight-node plane stress elements, with six-node line interface elements, and a maximum allowable tensile stress of 0.2 N/mm²); kinematic limit analysis (joints with unlimited compressive stress strength, zero tensile strength, and 37° for friction angle) and nonlinear finite elements analysis.

The arch dimensions are the following: a span of 5.0 m, a rise of 2.5 m, a thickness of 0.3 m, a width of 1.0 m, and a radius of 2.5 m with a backfill up to 3.0 m in height. The arch is subject to the action of its own weight, a filling and a concentrated variable load, which will be increased from a value of 10 kN to arch failure. The variable load is applied to 1/4 of the arch span. The characteristics for the material taken from [4] coincide with those described in Table 2 for the Cernadela Bridge arch, except the value of the Young's modulus, which is $E = 10 \cdot 10^3$ N/mm² in the first case. Table 4 shows the safety factors obtained by [4] for the different arch analyses.

Fig. 11 shows the geometric model used in the proposed method. In this case, the finite element discretisation of the arch voussoirs was performed with linear solid tetrahedra (4 nodes, with three degrees of freedom per node). Fig. 12 depicts the relationship between the live load versus displacements and maximum separation of voussoirs for the ideal regular arch computed with the proposed methodology. A sudden variation of the slope can be observed from the live load, which corresponds to failure. The failure load is estimated to be 20 kN.

The safety factor obtained is therefore $20/10 = 2$, were 10 kN is the initial live load considered in Ref. [4]. The differences with the results obtained with kinematic limit analysis and nonlinear finite element analysis performed by Loureço can be observed in Table 4.

If the kinematic analysis is taken for comparison as in the previous case, the result differs by 11% with the proposed numerical method. As in the arch in the Cernadela Bridge, the results are higher in the numerical method. The same remarks about the range of values for load failure as stated before may be considered here as well.

7. Summary and conclusions

This paper presents a multidisciplinary approach to documenting and evaluating a masonry bridge that integrates the results of close range digital photogrammetry, CAD tools and finite elements analysis (FEM). Photogrammetric techniques were used since they do not require direct contact with the arch for measurement, so they are not intrusive; further they are safe for workers because it does not require

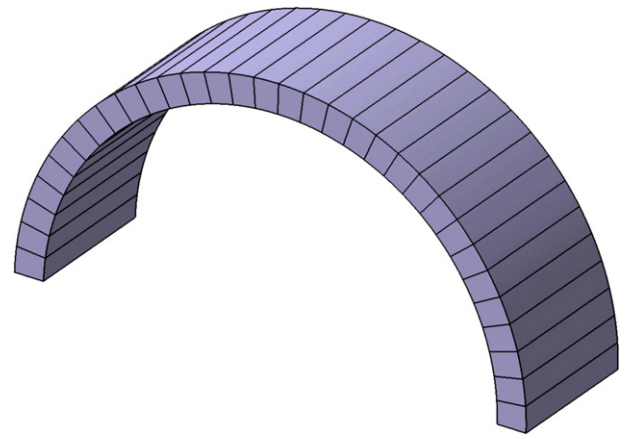


Fig. 11. Ideal model with regular geometry arch.

scaffolding; and they provide a geometric model that is closest to reality with high accuracy and detail in the geometry of each individual voussoir and set analysed. Close range photogrammetry was used to define a 3D cloud of points, where the points restituted in the contour of the bridge stones and their coordinates in the object space are obtained with millimetre accuracy. A full geometrical description of the entire bridge was obtained, including the span and rise of arches and the length and width of piers. A 3D wire frame model was obtained, which was further used to model each piece of the arches individually. The procedure to generate the solid model is described in detail. As a result, the geometry of the pieces of the arches is digitally reproduced precisely.

This geometric model with high fidelity was used for the mechanical analysis of one of the arches (the one with greater deformed shape) of the Cernadela Bridge (Galicia, Spain) using a discontinuous model of assembled voussoirs, which were discretised using finite elements without transmission of tension between contact surfaces. The failure live load of the studied external arch ring was obtained by calculating the load–displacement diagram through an iterative process. In addition, the stress distribution produced for this failure load was obtained at the interfaces and inside each individual voussoir.

The results for the proposed method were compared with an analysis of rigid blocks made in the Ring 2.0 software. In this last case, the arch geometry had to be simplified. It was found that the response of the proposed numerical method was qualitatively very similar to that obtained by rigid blocks with the formation of hinges in similar positions. The failure load in the numerical model with accurate

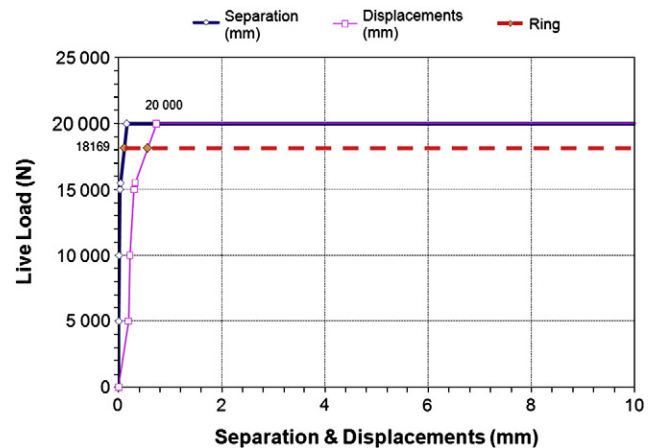


Fig. 12. Live load versus displacement and separation between voussoirs. Ideal model with proposed method.

Table 4
Safety factors for different analyses (Loureço, 2002).

Approach/analysis type	Safety factor
Allowable stresses ($f_{ta} = 0.2$ N/mm ²)	0.31
Kinematic limit analysis	1.8
$f_t = 0$, physical nonlinear	1.8
$f_t = 0$, physical and geometric nonlinear	1.7
$f_t = 0.2$ N/mm ² , physical nonlinear	2.5
$f_t = 0.2$ N/mm ² , physical and geometric nonlinear	2.5

geometry has proved to be higher by about 12% for the present case. It should be noted that the loss of stability occurs in the proposed method in a gradual process around a short range of load values, and accuracy can be increased by increasing the number of iterations made within this range.

In spite of a greater consumption of computational resources, the proposed methodology based on finite element analysis in discontinuous models provides interesting advantages for highlighting the failure load, safety factor or stress distribution in the interfaces and inside the voussoirs. These advantages are remarkable when the geometry of the arch is highly irregular or the voussoirs have a highly uneven shape.

Acknowledgements

The financial support of the Ministry of Science and Education (Spain) for Scientific Research under Grants No. BIA2006-10259 (Title: "Dimensional and structural analysis of constructions using close range photogrammetry, terrestrial laser and close range radar") and BIA2009-08012 (Title: "Observatory for masonry arch bridges: management system. OPAF-SIG"), and the grant for creation faculty staff (FPU) AP2006-04663 is appreciated.

References

- [1] K.H. Ng, C.A. Fairfield, Modifying the mechanism method of masonry arch bridge analysis, *Construction and Building Materials* 18 (2) (2004) 91–97.
- [2] A. Orduña, P.B. Lourenço, Three-dimensional limit analysis of rigid blocks assemblages. Part I: Torsion failure on frictional interfaces and limit analysis formulation, *International Journal of Solids and Structures* 42 (18–19) (2005) 5140–5160.
- [3] S. Huerta, Arcos, bóvedas y cúpulas: Geometría y equilibrio en el cálculo tradicional de estructuras de fábrica (*in spanish*) (Arches, vaults and domes: Geometry and equilibrium in the assesment of masonry structures), Instituto Juan de Herrera, Madrid, Spain, 2004.
- [4] P.B. Lourenço, Computations on historic masonry structures, *Progress in Structural Engineering and Materials* 4 (3) (2002) 301–319.
- [5] J. Heyman, The stone skeleton, *International Journal of Solids and Structures* 2 (1966) 249–279.
- [6] Heyman J. , *The masonry arch*, Ellis Horwood Ltd, 1982.
- [7] D. González-Aguilera, J. Gomez-Lahoz, A. Muñoz-Nieto, J. Herrero-Pascual, Monitoring the health of an emblematic monument from terrestrial laser scanner, *Nondestructive Testing Evaluation* 23 (4) (2008) 301–315.
- [8] C. Ordóñez, P. Arias, J. Herráez, J. Rodríguez, M.T. Martín, Two photogrammetric methods for measuring flat elements in buildings under construction, *Automation in Construction* 17 (5) (2008) 517–525.
- [9] A.H. Tyson, G.E. Mawdsley, M.J. Yaffe, Measurement of compressed breast thickness by optical stereoscopic photogrammetry, *Medical Physics* 36 (2) (2009) 569–576.
- [10] E.A. Leal, J. William, O. Ortega, Estimación de curvaturas y direcciones principales en nube de puntos no organizados, *Dyna* 74 (153) (2007) 351–362.
- [11] P. Arias, C. Ordóñez, H. Lorenzo, J. Herraéz, Methods for documenting historical agro-industrial buildings: a comparative study and a simple photogrammetric method, *Journal of Cultural Heritage* 7 (4) (2006) 350–354.
- [12] I. Lubowiecka, J. Armesto, P. Arias, H. Lorenzo, Historic bridge modeling using laser scanning, ground penetrating radar and finite element methods in the context of structural dynamics, *Engineering Structures* 31 (2009) 2667–2676.
- [13] L.M. Macareno, C. Angulo, D. López, J. Agirrebeitia, Analysis and characterization of the behaviour of a variable geometry structure, *Proceedings of the Institution of Mechanical Engineers. Part C: Journal of Mechanical Engineering Science* 221 (11) (2007) 1427–1434.
- [14] S. Franke, B. Franke, K. Rautenstrauch, Strain analysis of wood components by close range photogrammetry, *Materials and Structures/Materiaux et Constructions* 40 (1) (2007) 37–46.
- [15] P. Arias, J. Armesto, D. Di-Capua, R. González-Drigo, H. Lorenzo, V. Pérez-Gracia, Digital photogrammetry, GPR and computational analysis of structural damages in a mediaeval bridge, *Engineering Failure Analysis* 14 (8) (2007) 1444–1457.
- [16] L. Schueremans, B. Van Genechten, The use of 3D-laser scanning in assessing the safety of masonry vaults—a case study on the church of Saint Jacobs, *Optics and Lasers in Engineering* 47 (3–4) (2009) 329–335.
- [17] A.M.C. Sonnenberg, R. Al-Mahaidi, Investigation of dowel shear in RC beams using photogrammetry, *Magazine of Concrete Research* 59 (9) (2007) 621–626.
- [18] S.O. Mason, Conceptual model of the convergent multistation network configuration task, *The Photogrammetric Record* 15 (86) (1995) 277–299.
- [19] D.V. Jauregui, K.R. White, J.W. Pate, C.B. Woodward, Documentation of bridge inspection projects using virtual reality approach, *Journal of Infrastructures Systems* 11 (3) (2005) 172–179.
- [20] Cooper M. , Robson S. , *Theory of Close Range Photogrammetry*, in: Atkinson K.B. (Ed.), *Close Range Photogrammetry And Machine Vision*, Whittles Publishing, Caithness, Scotland, 2001, pp. 9–51.
- [21] W. Zhizhuo, *Principles of Photogrammetry*, Publishing House of Surveying and Mapping, Beijing, 1990.
- [22] P. Arias, J. Herraéz, H. Lorenzo, C. Ordóñez, Control of structural problems in cultural heritage monuments using close-range photogrammetry and computer methods, *Computers & Structures* 83 (21–22) (2005) 1754–1766.
- [23] P.R. Wolf, B.A. Dewitt, *Elements of Photogrammetry with Applications in GIS*, McGraw-Hill, EEUU, 2000.
- [24] P. Arias, J.C. Caamaño, H. Lorenzo, J. Armesto, 3D modelling and section properties of ancient irregular timber structures by means of digital photogrammetry, *Computer-Aided Civil and Infrastructure Engineering* 22 (8) (2007) 597–611.
- [25] C. Greve, *Digital Photogrammetry: An Addendum to the Manual of Photogrammetry*, ASPRS, Bethesda, Maryland, EEUU, 1996.
- [26] A. Kooharian, Limit analysis of voussoir (segmental) and concrete arches, *Journal American Concrete Institute* 24 (1952) 317–328.
- [27] R.K. Livesley, Limit analysis of structures formed from rigid blocks, *International Journal for Numerical Methods in Engineering* 12 (1978) 1853–1871.
- [28] M. Gilbert, On the analysis of multi-ring brickwork arch bridges, *Proc. 2nd International Arch Bridges Conference, Venice, 1998*, pp. 109–118.
- [29] A. Munjiza, *The combined finite-discrete element method*, John Wiley & Sons, 2004.
- [30] Micron, CMOS Image Sensors, <http://www.micron.com/products/imaging>, last access May 2009.
- [31] Ring 2.0 Theory & Modelling Guide, LimitState. Sheffield, UK. Available at: <http://www.limitstate.com/ring>.
- [32] F. Fernandes, Evaluation of two novel NDT techniques: microdrilling of clay bricks and ground penetrating radar in masonry, Ph.D. thesis, Universidade do Minho, Portugal, 2006.
- [33] M. Solla, H. Lorenzo, F.I. Rial, A. Novo, B. Riveiro, Masonry arch bridges evaluation by means of GPR, *Proceedings of 13th International Conference on Ground Penetrating Radar, 2010*, pp. 394–399.
- [34] C. Colla, P.C. Das, D. McCann, M. Forde, Sonic, electromagnetic and impulse radar investigation of stone masonry bridges, *NDT&E International* 30 (1997) 249–254.
- [35] Z. Orbán, M. Gutermann, Assessment of masonry arch railway bridges using non-destructive in-situ testing methods, *Engineering Structures* 31 (2009) 2287–2298.